Materials Research Proceedings 31 (2023) 324-335 https://doi.org/10.21741/9781644902592-34

Estimation of failure load of adhesively bonded composite joints with embedded crack in adherends: bond EM

JAMES Polagangu[1,a*], BYJI Varughese[1,b]

[1]Advanced Composites Division, CSIR National Aerospace Laboratories, Bangalore, India

[a] james@nal.res.in*, [b] byji@nal.res.in

Keywords: Composite Structures, Failure load, Bonded Joints, Delamination, Crack, Bond Energy Method

Abstract. The authors developed Bond Energy Method (Bond EM), a novel quasi-numerical-analytical failure estimation method based on the energy conservation principle. This method previously estimated the ultimate failure load of adhesively bonded composite (ABC) repaired joints of third-party experiments without crack. In this present study, authors used the same method to estimate the ultimate failure load of third-party ABC joint test specimens with an embedded crack in the adherends. The adhesive layer and adherends are modeled using one and two-dimensional finite elements in such a way that *one plus two is three* to capture three-dimensional stresses. The crack in adherend is modeled by adding a Teflon layer of 0.02 mm between its composite stacking sequence. Static stress analysis is carried out to obtain the precise force and stress values in the adhesive layer and adherends per unit load (1000 N). These values are appropriately substituted in mathematical equations of Bond EM and estimated the ultimate failure load of L. Tong's test specimens. The difference in mathematical estimation is found in the range of (+4.29, +18.15)% for higher side estimation; (-4.80, -34.50)% for lower side estimation. The study compared the estimated failure load by Bond EM with that of other popular third-party methods, and Bond EM is found superior to all other methods considered in this study.

1. Introduction

Council of Scientific and Industrial Research-National Aerospace Laboratories (CSIR-NAL) Bangalore is a premier scientific research institute funded by the Government of India, engaged in the design, development, manufacturing, and certification of both military and civil transportation category aircraft. Advanced Composites Division of CSIR-NAL carries out research on the design and development of lightweight composite structures. The composite parts may show the deviations such as delamination, damage, resin rich, resin starved areas, and uninvited foreign debris in the composite laminate region. These deviations pose a serious technical challenge to the designer for acceptance of the part. Understanding the effect of such deviations on the overall performance and structural integrity of composite parts became the subject of interest for composite structural designers. Several analytical models are available for understanding the failure of a composite laminate of test coupons, however, those methods cannot be implemented on a global two-dimensional finite element model with induced delamination, or crack. Therefore, the authors developed an innovative and simplified finite element analysis procedure for modeling ABC joints with an embedded crack in composite laminate; and mathematically estimated the ultimate failure load of such joints using Bond EM [1]. Authors developed this method to understand analytically the effect of a manufacturing defect in bigger composite parts. Authors estimated the ultimate failure load of third-party ABC joints without crack; which was designed using various material distribution, size, and shape subjected to both uniaxial tension and compression loading. In the present study, the same method is used in its original form to estimate the ultimate failure load of ABC joints with the embedded crack in the adherends. The details of

ABC joints considered in the present study have reference to the experimental models tested by L. Tong in 1998 [2] with the embedded crack in adherends.

2. Literature

Without conducting any experiments, it is difficult to estimate the ultimate failure load of ABC joints using allowable material strength properties of the adhesive layer and adherends. Prediction of progressive failure of bonded joints through a conventional material strength approach is not possible. James Polagangu *et al* [1] made it simple to estimate the ultimate failure load of such ABC joints through a novel FE modeling approach and Bond EM; validated the method using *third-party* experimental results referenced by various researchers [3-5]. Phil Yarrington *et al.* [6] carried out the analytical study to validate L. Tong's experimental models [2] using Linear and Nonlinear HyperSizer finite element analysis tools. But, this method could predict the first failure load of L. Tong's experimental specimen of group A without a crack in adherend. He reported that these HyperSize analyses ended the solutions due to the singularity problems encountered because of the modeling of cracks in three-dimensional finite element models; therefore, not reported the estimated failure loads of other groups of specimens from B to F.

2.1. Status of failure theories

M. J. Hinton *et al.* [7] carried out a worldwide review exercise with the title *World Wide Failure Exercise* on 12 leading failure theories popularly known to predict the failure of composite laminates. The team carefully selected 14 test cases, contacted the originators of failure theories, and collected the necessary information on test data to predict the failure. The exercise avoided the information on theoretical and test data from third-party researchers. This exercise summarized the weakness and strengths of all leading failure theories by comparing the theoretically predicted failure load and test data. This worldwide exercise concluded that *a huge gap* existed between theoretical predictions and experimental data. Therefore, the mechanics of composite laminates, composite structures, composite co-cured T-joint, and ABC joints is still an open-ended research area. James Polagangu *et al.* [8] developed a simplified finite element modeling approach to understand the stress distribution around Bermuda Triangle (BT) region in the composite co-cured T-joint intersection. The load-carrying capacity of such a complex composite joint was explained through a novel failure criterion, and showed compliance with airworthiness certification requirements.

2.2. Material science and engineering at a glance

The concept of stress, strain, and elasticity explains the overall material strength, behavior, and structural mechanics of small prismatic member to large structures. The name of Scientists and year of discovery [9,10, 11] of various basic material engineering parameters is briefly summarised for ready reference. Understanding the subject of material science and engineering, mechanics of structures, and failure mechanics took centuries of the period to add a new engineering parameters like stress, strength, stiffness, and mechanical energy terms.

Sir Robert Hooke proposed the law of linear elasticity of material within the proportional limit, named Hooke's law in 1660, and published in 1678 (*17th Century*). Gottfried Wilhelm Leibniz in 1684, and Jakob Bernoulli in 1691 explained the idea of internal tension acting across the surface in a deformable solid. In 1705 (*18th Century*), Jakob Bernoulli observed and described the deformation through force per unit area or stress. In 1727, Leonhard Euler proposed a linear relationship between stress σ and strain ε. In 1752, Euler introduced the idea of compressive normal stress as the pressure in a fluid. For the first time, Charles-Augustin Coulomb introduced the theory of a beam as a bent elastic line; and related the bending to stress and strain in an actual beam, he developed the famous expression $\sigma = (M/I)y$ for the stress due to the pure bending of a homogenous linear elastic beam. In 1782, Giordano Riccati performed the first experiments similar to the concept of Young's modulus. Charles Augustin Coulomb correctly formulated the entire

problem of cantilever beam bending in a paper published in 1773. But, In 1807 (*19th Century*), Thomas Young related the stress and strain in the form σ=Eε. There appears to be a timeline disparity between the above two time periods, however, it is considered to be insignificant from the present contest. Euler–Bernoulli published the beam theory for the first time in 1750 but it became popular only in the 19th century during erection of the Eiffel tower in 1887 due to its validation. Therefore, it is understood that it took almost two centuries from the time of Hooke's law to erection of the Eiffel Tower, 1660 to 1887, to understand, formulate and validate the simple theory of bending equation M/I=f/y=E/R. In 1713, Antoine Parent introduced the concept of shear stress. In 1773, Coulomb developed this concept further, explained the failure of solids in connection with the stressing beams; and studied frictional slips in 1779. This literature review convinces us that any mathematical, analytical /numerical method developed by one scientist should be validated by the work of another scientist/ experimentalist /designer. Therefore that particular method can be used by other designers for designing large structures. The present paper also aimed at validating the Bond EM through third-party experimental results and proving its adaptivity for any type of ABC joints.

2.3. Bond energy method

James Polagangu *et al.* mathematically formulated Bond EM [1], a novel failure estimation formulation developed based on mass and energy conservation laws.

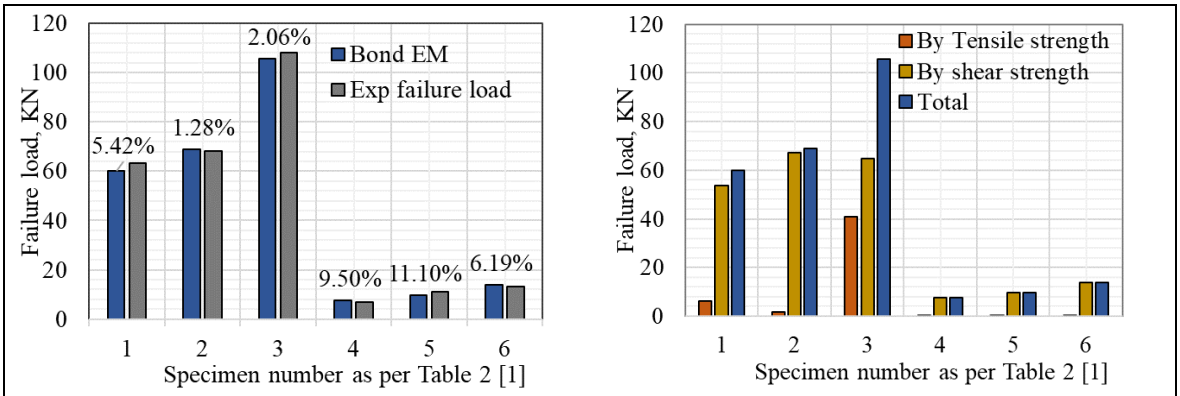

(a) Percentage difference between the ultimate failure load estimated by Bond EM and the experimental failure load of third-party test specimens

(b) Ultimate load resisted by allowable tensile and shear strength properties of the adhesive layer estimated by Bond EM

Figure 1. Failure load estimated by Bond EM and third-party test results. Refer Table 2[1]

The mathematical form of this method consists of widely known basic mechanical strain energy terms such as $\sigma^2/2E$ and $\tau^2/2G$ with an additional new term named Bond energy $\tau^2/2E$. The original work of this method explained the structural behavior of ABC joints of various popular configurations through a simplified one and two-dimensional finite element modeling approach. For the first time, this method estimated the failure load of ABC repaired joints [3-5] of different sizes, shapes, and materials subjected to both tensile and compressive loads. The lowest difference in mathematical estimation was 1.28%, as shown in Fig.1(a). Figure. 1(b) shows the uniqueness of Bond EM. The method quantifies the load carried by the allowable tensile and shear strength properties of the adhesive layer separately. Most of the specimens predominantly failed in shear except the 3rd specimen, which resisted the applied load considerably by tensile strength property of the adhesive layer. The vertical face of the stepped bonded joint configuration consumed the internally stored tensile strain energy from the adhesive layer, which satisfies the general understanding of the structural behavior of ABC joints of that configuration.

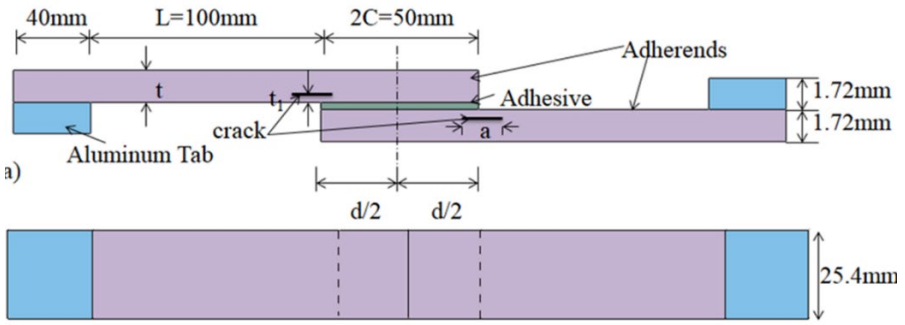

(a) Geometrical configuration of L. Tong's specimens

Summary of geometrical dimensions of six specimens

Experimental group	A	B	C	D	E	F
a, crack width in mm	0	4	6	8	6	6
d, offset distance in mm	50	50	50	50	60	40

(b)Left hand side adherend and tab

(c) Right hand side adherend and tab

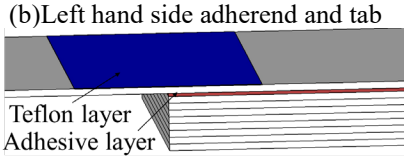

(d) Adhesive layer and crack in upper adherend

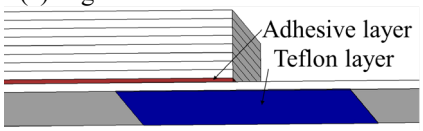

(e) Adhesive layer and crack in lower adherend

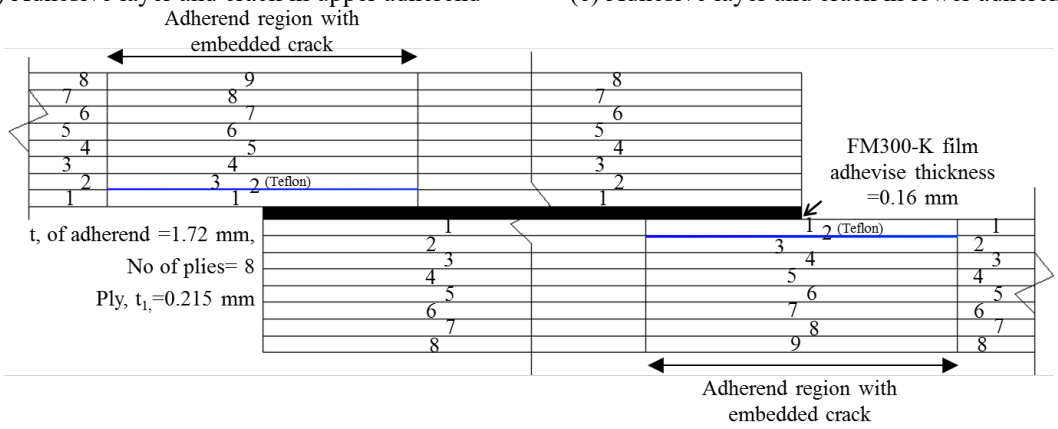

(f) Stacking sequence details around the embedded crack region

Figure 2. Geometrical details of L. Tong's experimental models [2]

3. ABC Joints with the embedded crack in Adherends

The present study aims at estimation of the failure load of ABC joints with the embedded crack in the adherends, however, determination of deflection, rotation, and conducting nonlinear progressive failure analysis of such joints is beyond the scope. The experimental studies carried out by L. Tong in 1998 [2] with the embedded crack in both adherends are the reference models considered in the study. Figure 2 shows the geometrical dimensions of L. Tong's specimens, with the crack embedded at the second layer of each adherends with different sizes and positions.

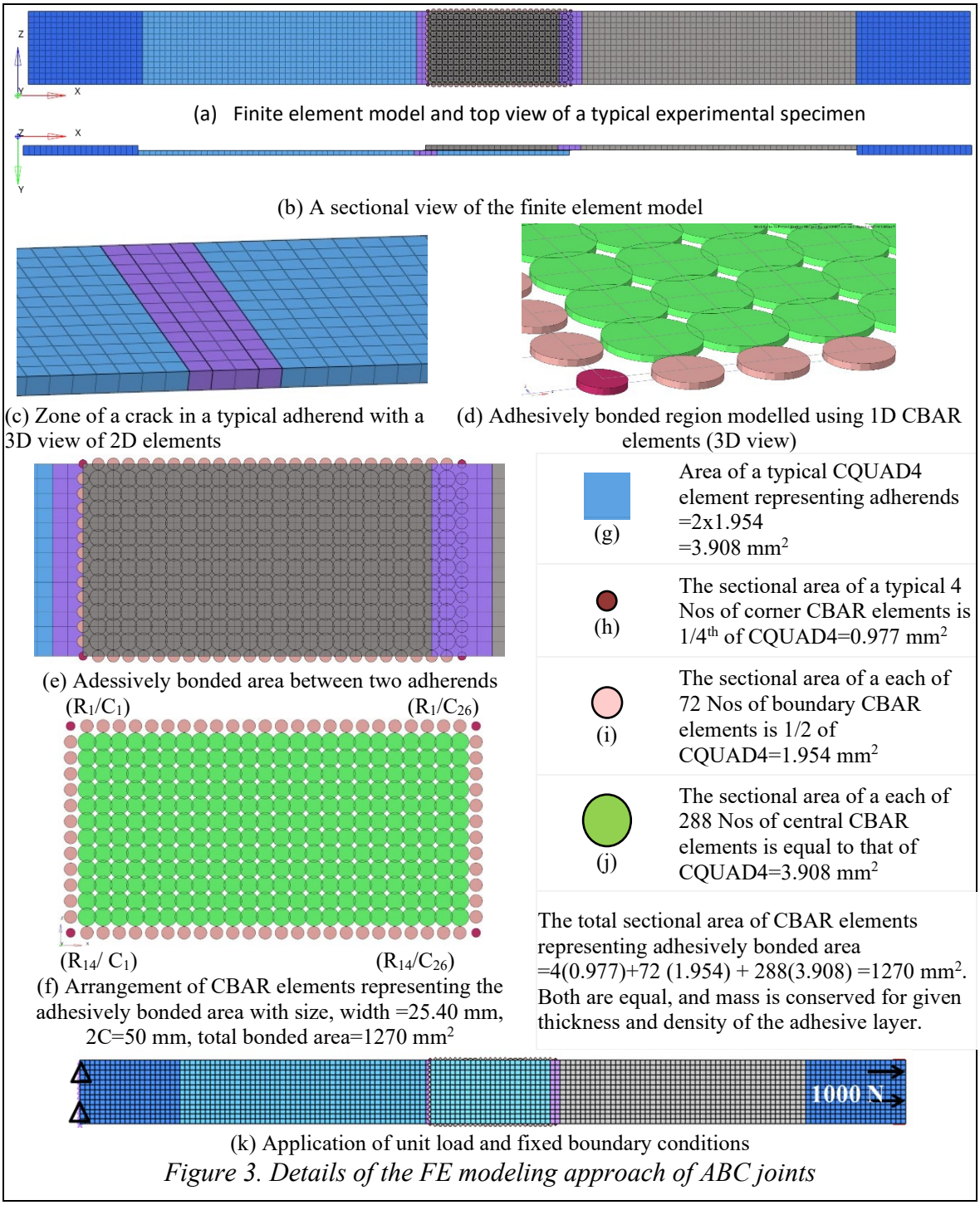

Figure 3. Details of the FE modeling approach of ABC joints

3.1. Finite element model

The authors explained the procedure for creating one and two-dimensional finite element models of ABC joint [1]. The present study adopted the same approach for creating such models with the embedded crack using Hypermesh® Pre- and Post Processor. The top view of a typical specimen model is shown in Fig.3(a). The adherend region with and without crack is shown in Fig.3(b)&(c). The adherends are modeled using 2D-CQUAD4 elements with PCOMP property, MAT8 material cards; and the adhesive layer is modeled using ID-CBAR beam elements of NASTRAN® element library defined by PBARL property card with the circular sectional area as shown in Fig.3(d). The arrangement and sectional area of elements are shown in Fig.3(f) to (j) respectively. The adhesive

layer surface area is 1270 mm^2, and that of CBAR elements is 1270 mm^2, which confirms the conservation of mass from a single surface to multiple CBAR sectional areas. These elements have all six degrees of freedom to capture the force components along three axes, and bending moment about three axes that arise due to the eccentricity of a single lap joint. The composite stacking sequence of both adherends consists of eight plies of $(0^o)_8$ orientation as per the layup details marked in Fig. 2(f). The composite stacking sequence of adherend includes a Teflon film layer of 0.02 mm (t_1) embedded by adding a layer at the position shown in Fig. 2(a),(d) to (f). The Teflon layer defined by the fictitious isotropic material properties (E=0.55 GPa, and υ=0.3) virtually represents and simulate the condition of the crack in adherend. The finite element model for six specimens is created with appropriate crack dimension and position as per the summary given in Fig.2. Figure 3(k) shows loading conditions applied to the finite element models. The top adherend is constrained against all rotation and translations; a unit load of 1000 N is applied at another end of the bottom adherend that pulls the joint away from the bonded region.

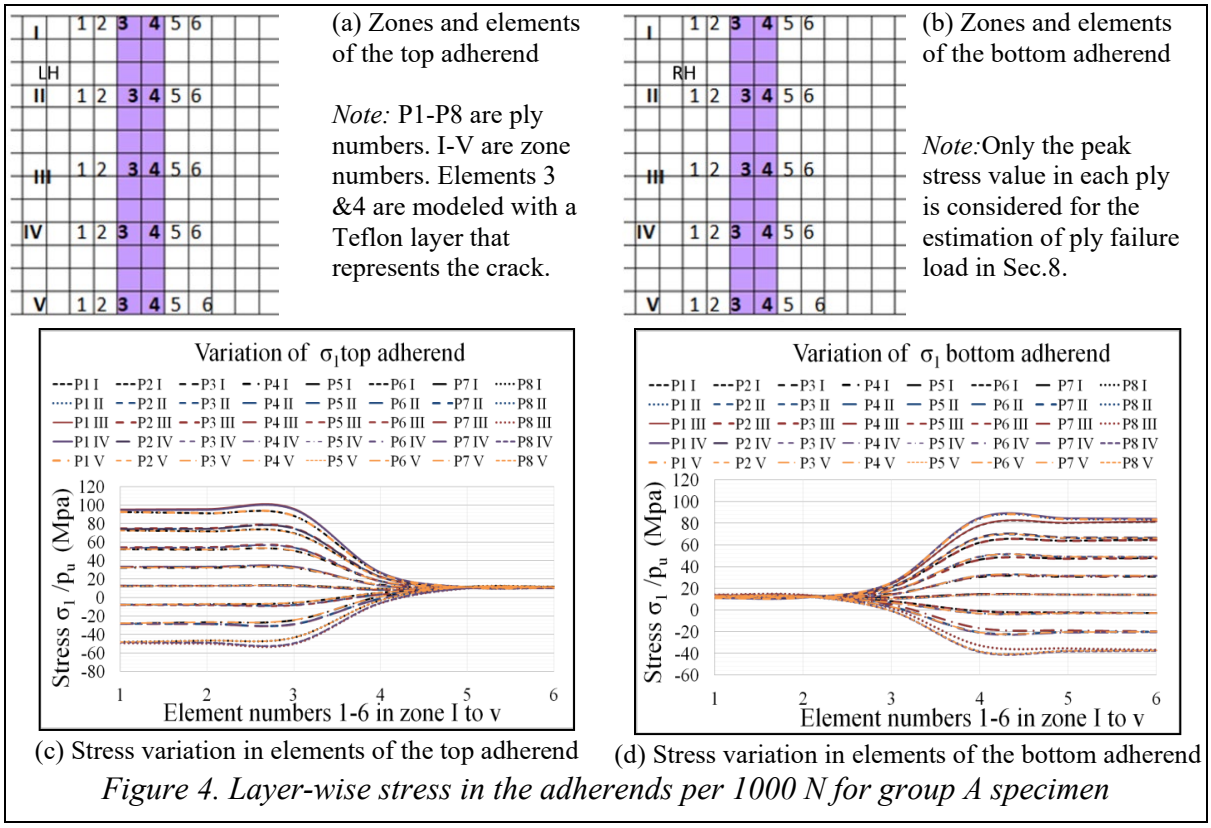

(a) Zones and elements of the top adherend

Note: P1-P8 are ply numbers. I-V are zone numbers. Elements 3 &4 are modeled with a Teflon layer that represents the crack.

(b) Zones and elements of the bottom adherend

*Note:*Only the peak stress value in each ply is considered for the estimation of ply failure load in Sec.8.

(c) Stress variation in elements of the top adherend

(d) Stress variation in elements of the bottom adherend

Figure 4. Layer-wise stress in the adherends per 1000 N for group A specimen

4. Analysis and Results

4.1. Stress in the composite plies of adherends

The static stress analysis is carried out using MD Nastran® solver for all six models. The analysis called for output data of composite ply-wise stresses and force components for all CBAR elements. The output data is post-processed outside the analysis domain using a Microsoft® Excel spreadsheet inline with the CBAR element position marked in rows R_i (*i=1 to 14*) and columns C_j (j=1 to 26) as shown in Fig.3(f); zones I to V and element numbers 1 to 6 marked for both adherends as shown in Fig.4 (a)&(b). The ply-wise stress distribution in those elements located near to the crack region is shown in Fig. 4(c)&(d) for both top and bottom adherends respectively w.r.t the zones and number of elements marked in the same figure. The ply-wise stress distribution shows that the 1st layer of 3rd element in zone IV attains maximum tensile stress of 95.51 MPa and

the 8th layer of 3rd element in zone IV linearly attains the maximum compressive stress of -49.59 MPa due to known eccentricity in single lap joint configuration. Similar observations are made for another group of specimens with a significant changes in the stress values.

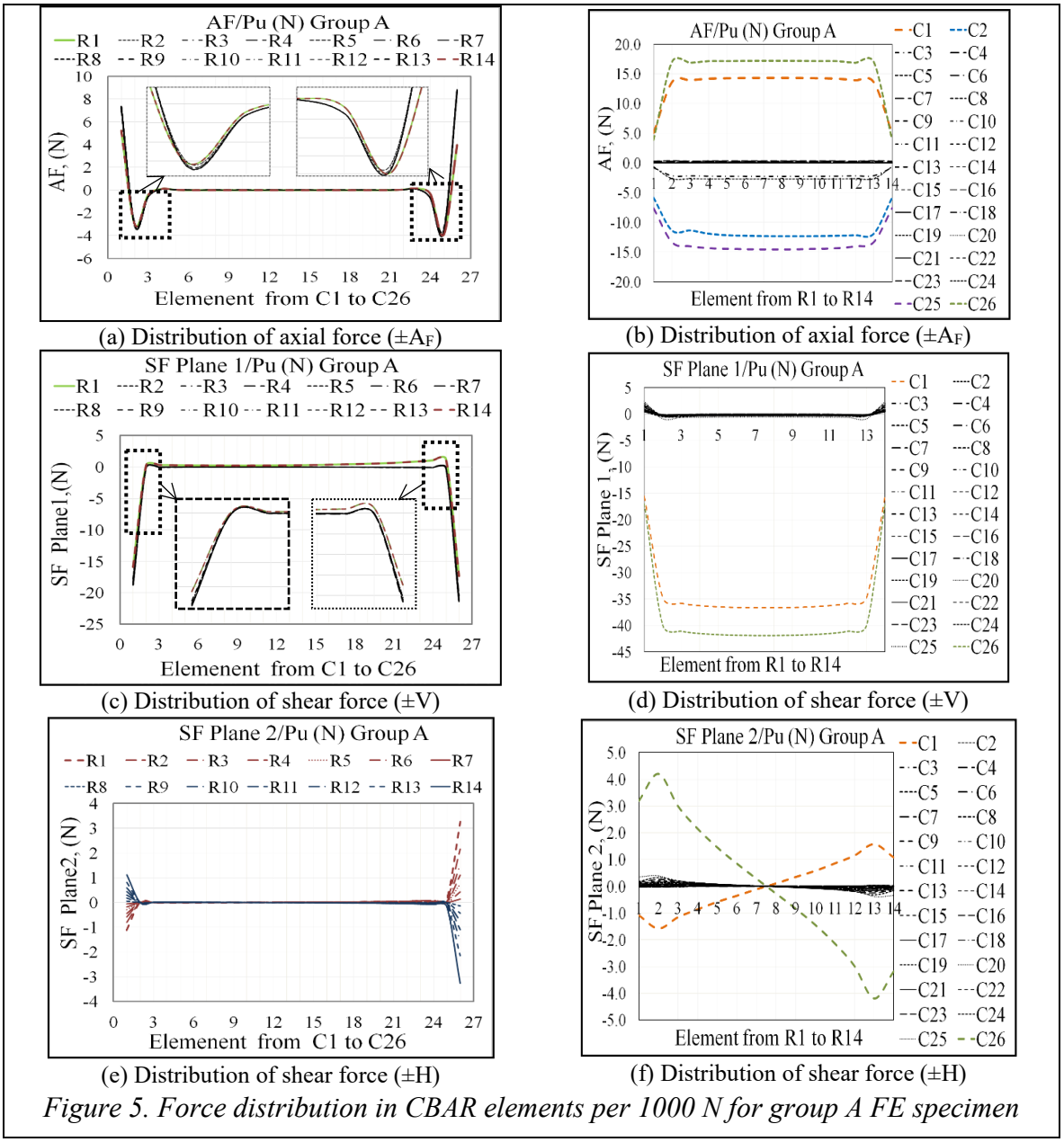

(a) Distribution of axial force (±A_F) (b) Distribution of axial force (±A_F)

(c) Distribution of shear force (±V) (d) Distribution of shear force (±V)

(e) Distribution of shear force (±H) (f) Distribution of shear force (±H)

Figure 5. Force distribution in CBAR elements per 1000 N for group A FE specimen

4.2. Force in the adhesive layer

Figure 5(a) to (f) shows the force distribution in CBAR elements per 1000 N for a typical group A experimental specimen. The force component divided by the respective sectional area of that element gives the stress value in the respective direction. The sense of axial force (AF) is denoted by ±AF, where +AF is axial tension and –AF is axial compression force in the adhesive layer which is acting normal to the adherend. Force components acting in the direction of applied load or material orientation of the adherends is denoted by ±V w.r.t the direction of applied force or vector *v1* of CBAR element. Force components acting in the plane of the adhesive layer and transverse direction to the applied load is denoted by ±H or w.r.t the vector *v2* of CBAR element.

Materials Research Proceedings 31 (2023) 324-335 https://doi.org/10.21741/9781644902592-34

Force distribution shows that those elements located around the boundary of the adhesive layer experience high out-of-plane force or stress for all models.

5. Ultimate failure load estimation by Bond EM

5.1. Ultimate failure load of adhesive layer

Force components are converted into equivalent stress values in respective CBAR elements. The same stress values are appropriately substituted in Eq.1 to Eq.3. The allowable tensile strength property of the adhesive layer stores the tensile strain energy F_T in the form of $(\sigma^2/E)_{ij}$, in all elements that are exclusively subjected to tensile stress as given in Eq.2. The allowable shear strength property of the adhesive layer stores the shear strain energy F_S in the form of $(\tau^2/G)_{ij}$, in all elements that are exclusively subjected to shear stress in both longitudinal and transverse directions as given in Eq.3. While those CBAR elements that are exclusively subjected to compressive load stores the Bond energy in the form of $(\tau^2/E)_{ij}$ as given in Eq.3.

The ultimate failure load of ABC joints is defined by $$F_{ufl}^{Ad} = \frac{P_U^2}{n_b}\left[F_{ufl}^{T} + F_{ufl}^{Sh}\right] \quad (1)$$

Where,

$$F_T = F_{ufl}^{T} = \left(\frac{\sum_{i=1}^{n}\sum_{j=1}^{m}\left(\sigma_{z,al.}^2 a_a.t_a / E_a\right)_{ij}^{+A_F}}{\sum_{i=1}^{n}\sum_{j=1}^{m}\left(\sigma_{y,ap}^2 a_a.t_a / E_a\right)_{ij}^{+V} + \sum_{i=1}^{n}\sum_{j=1}^{m}\left(\sigma_{y,ap}^2 a_a.t_a / E_a\right)_{ij}^{-V} + \sum_{i=1}^{n}\sum_{j=1}^{m}\left(\sigma_{z,ap}^2 a_a.t_a / E_a\right)_{ij}^{+A_F} + \sum_{i=1}^{n}\sum_{j=1}^{m}\left(\sigma_{z,al} a_a.t_a / E_a\right)_{ij}^{-A_F}} \right) \quad (2)$$

$$F_S = F_{ufl}^{Sh} = \left(\frac{\sum_{i=1}^{n}\sum_{j=1}^{m}\left(\tau_{xy,al}^2 a_a.t_a / E_a\right)_{ij}^{-A_F} + \sum_{i=1}^{n}\sum_{j=1}^{m}\left(\tau_{yz,al}^2 a_a.t_a / G_a\right)_{ij}^{+H} + \sum_{i=1}^{n}\sum_{j=1}^{m}\left(\tau_{yz,al}^2 a_a.t_a / G_a\right)_{ij}^{-H}}{\sum_{i=1}^{n}\sum_{j=1}^{m}\left(\tau_{yz,ap}^2 a_a.t_a / G_a\right)_{ij}^{+H} + \sum_{i=1}^{n}\sum_{j=1}^{m}\left(\tau_{yz,ap}^2 a_a.t_a / G_a\right)_{ij}^{-H}} \right) \quad (3)$$

NOTE: Wherein P_u is the number of unit loads applied. If the applied load is 1000 N, then P_u=1. If the applied load is 10,000 N, then P_u =10. The numerical value of n_b is equal to the number of bonded faces, n_b =1 for one side bonded joint, n_b =2 for two sides bonded joint. *Nomenclature*: σ tensile stress, τ shear stress, a_a cross sectional area, t_a thickness, E_a Young's modulus, and G_a shear modulus of respective CBAR element.

Ultimate failure load is the load required to fail the adhesive layer or composite plies completely so that it separates both the adherends. This condition occurs when two criteria are satisfied. The first criterion is satisfied when externally applied load or tensile stress consumes the internally stored tensile strain energy F_T of the adhesive layer. The second criterion is satisfied when externally applied load in the form of shear stress consumes the internally stored shear strain energy F_S. The ABC joint sees both tensile and shear stress regions due to complex structural details and loading conditions. Therefore, the total ultimate failure load is the sum of two strain energy terms $F_T + F_S$ respectively. Figure 6 shows the comparison of the ultimate failure load of Tong's experimental specimens with that of Bond EM. L. Tong had not reported the ultimate failure load of all five specimens of groups A and F due to large variations in failure load [2].

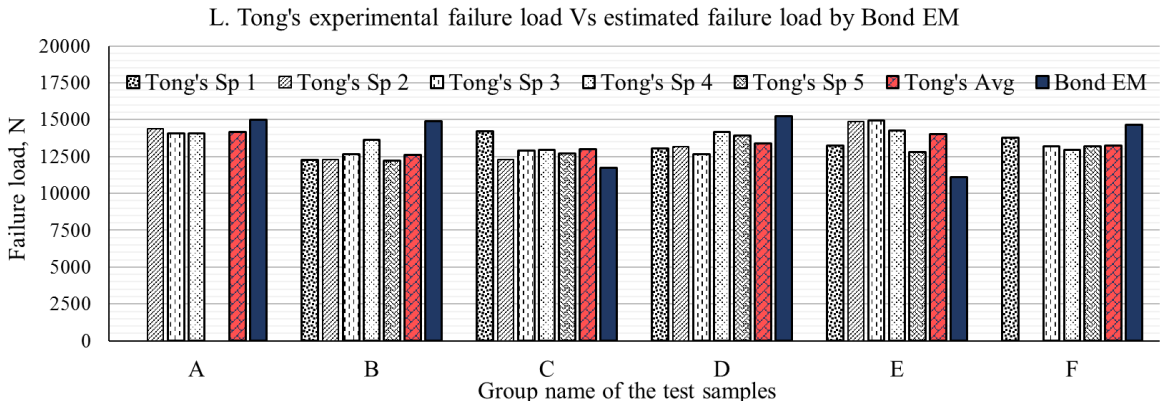

Figure 6. Comparison of failure load estimated by Bond EM with that of Tong's experimental models [2]

5.2. Comparison of failure load

Table 1 gives the summary of the ultimate load estimated by Bond EM. The percentage difference is estimated w.r.t maximum, minimum, and average ultimate failure load value of experiment models. It shows that the load estimated by Bond EM differs by +4.29%, 18.15% for group A and B specimens; -4.80%, and -34.50% for group C and E specimens respectively. The positive difference indicates the estimated failure load is higher than experimental values and Vice-Versa. The higher difference between the minimum and maximum values indicates the larger variation in the experimental failure load of specimens of that group.

Table 1. Summary of ultimate failure load estimated by Bond EM

S. No	Name of specimen group	A	B	C	D	E	F
[1]	*[2]*	*[3]*	*[4]*	*[5]*	*[6]*	*[7]*	*[8]*
1	Failure load by Bond EM, N	15018	14917	11718	15242	11114	14674
2	The difference with minimum load (%)	*4.29*	8.64	*-4.80*	7.01	-15.28	6.14
3	The difference with maximum load (%)	6.35	*18.15*	-21.32	16.89	*-34.50*	11.93
4	The difference with the average load (%)	5.64	15.55	-10.97	12.11	-26.15	9.62

5.3. Reason for higher difference

The higher difference between the experimental and estimated failure loads attribute to various parameters that influence the manufacturing and testing procedure. The temperature, pressure, and duration of curing affect the quality of the specimen. The variation in thickness of the adhesive layer and the inclusion of foreign debris sometimes may reduce the failure load. The present study considered the uniform thickness of the adhesive layer throughout the bonded region as defined[2]. The study assumed perfect compactness of the joint with no manufacturing defects induced in both the adhesive layer and adherends. These assumptions have resulted in the higher prediction of failure load as seen in groups A, B, D, and F; for the other two groups C and E, the prediction is on the lower side. The lower prediction of failure load is attributed to the possible deviation of experimental specimens[2] from the standard dimensions. Authors report based on experience that the specimens with deviation were found to take a higher load than the pristine specimens. A good practice is to report any deviation/defect in the experimental specimens, as the Bond EM understands the structural behavior of ABC joints with such deviations.

7. Bond EM versus other methods

L. Tong [2] predicted the failure load of test specimens using maximum stress criterion FEA-MSC, energy release criterion ERC, and other theoretical methods. Phil Yarrington [6] also predicted the

failure load of L. Tong's test specimens using initial failure load, HyperSizer Linear, and Nonlinear methods. The ultimate failure load predicted by various analytical models, including Bond EM, with that of the average failure load of respective specimen groups is shown in Fig.7.

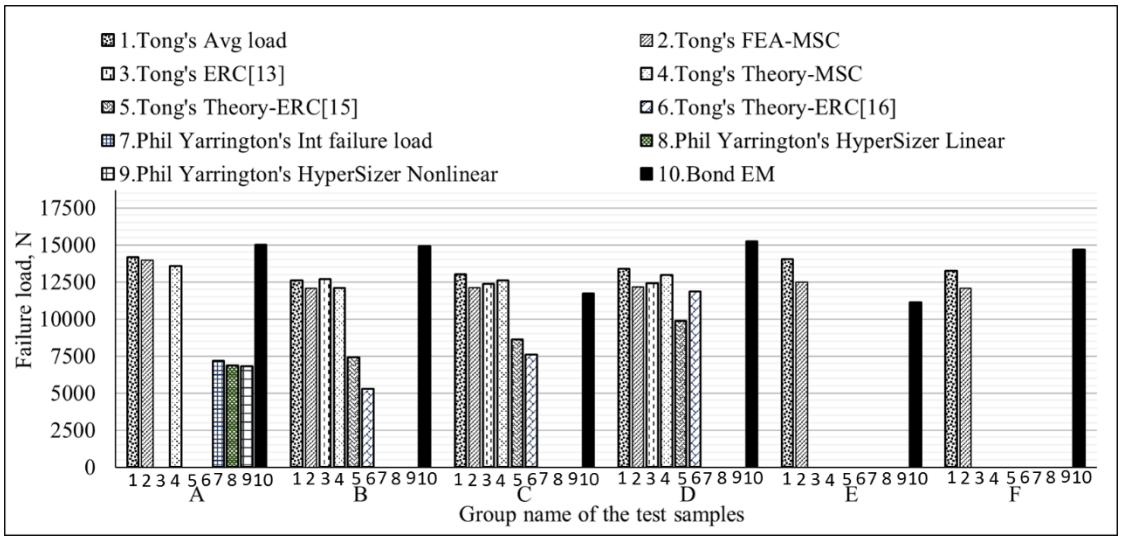

Note: References [13,15,16] from [2,6]

Figure 7. Comparison of Tong's failure load estimated by various analytical models and Bond EM

The failure load predicted by L. Tong using FEA-MSC closely correlated to the own experimental specimens of all groups, but the failure load predicted by other third-party methods is comparable with a few groups of specimens with a large gap. Phil Yarrington [6] estimated the first ply failure load of group A-specimens with a considerable variation but not reported for other groups of specimens as the singularity error encountered while solving ABC joint with crack. The present study also predicted the ultimate failure load of all groups of specimens with the variations discussed in *Sec 5.3*. The one and two-dimensional finite element modeling approach adopted in this study never encounter reported *singularity* error. This comparison reveals that Bond EM is *superior* to all analytical and theoretical methods discussed in this paper as it also predicted the failure load of all ABC joints with cracks.

8. Linear progressive failure analysis

Section 5.1 discussed the method of estimating the ultimate failure load of an adhesive layer of all groups of test specimens. In this section, a simple mathematical linear progressive analysis is carried out to understand the load at which a particular composite ply of adherend failed. The in-plane tensile stress value per unit load along with the allowable tensile strength property is sufficient for estimating the ultimate load at which the composite plies failed in sequence / progressively. For the demonstration purpose of this approach, the study considered the composite ply in-plane stress distribution in the top adherend of group A specimen as shown in Fig.4(c). Table 2 gives the sequence of simple mathematical calculations performed to estimate the ultimate failure load of each composite ply. L. Tong's [2] experimental models showed that composite plies simultaneously failed along with the adhesive layer. Phil Yarrington *et al* [6] determined the margin of safety values available in the composite plies of L. Tong's experimental models using HyperSizer 3D finite element analysis. The present study estimated and explained the sequence of failure of composite plies and the adhesive layer, and a numerical value of the failure load of each ply is reported in Table 2. Similarly, the peak in-plane tensile stress values in the composite plies of other specimen groups govern the failure. The first failure occurred in the composite ply adhered to the adhesive layer, and the failure progressed towards the free surface until the adhesive layer

ultimately failed. Both top and bottom adherends exhibited this phenomenon simultaneously. Figure 8 shows the path of failure across the thickness of adherends and the adhesive layer, which is in agreement with the reported failure mode[2].

Table 2. Estimation of failure load and mode of failure (for group A specimen)

Ply No	Ply stress per 1000 N, MPa *Refer Fig. 4(c)*		Ply failure load, N		Description of failure
	Top Adh	Bot. Adh	Top Adh	Bot. Adh	
1	*2*	*3*	*4*	*5*	*6*
Ply 1	95.51	84.15	5423	6156	Tensile failure*
Ply 2	75.35	66.66	6875	7771	Tensile failure*
Ply 3	54.41	49.18	9520	10533	Tensile failure*
Ply 4	33.46	31.69	**15481**	16346	Adhesive failure**
Ply 5	12.73	14.38	-	-	No failure++
Ply 6	-8.13	-3.28	-	-	No failure ++
Ply 7	-28.86	-20.76	-	-	No failure ++
Ply 8	-49.59	-38.24	-	-	No failure++

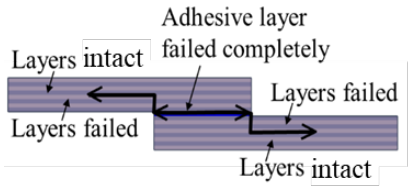

Figure 8. Schematic representation of failure mode in both adhesive layer and adherends

NOTE: (1) In-plane tensile strength of composite ply is 518 MPa [2,3]; (2) Value in column 4 =1000x 518 / Value in column 2; (3) Value in column 5 =1000x 518 / Value in column 3; (*) Ply failure initiated only at the highly stressed region, but plies continued to taking load along with other plies and adhesively layer; (**) The joint failed due to the separation of the adhesive layer; (++) the failure was not initiated in these plies but continued taking load along with other plies and the adhesive layer. Further investigation is needed to work out the load at which the individual ply fully failed across the width. Ply 4 in the top adherend and adhesive layer failed simultaneously. Difference in estimation of the ultimate failure load by this mehod is only 3.08% (=15481/15018-1)%.

9. Conclusions

This paper discussed the Bond Energy Method, finite element modeling approach, and method of estimating the ultimate failure load of adhesively bonded composite joints with embedded cracks. The method estimated and validated the ultimate failure load of L. Tong's experimental specimens of various groups with a crack embedded in both the adherends with a close correlation within the range of (+4.29, +18.15)% for higher side estimation; (-4.80, -34.50)% for lower side estimation, which is the closest estimation of all other methods. The comparison showed that Bond EM is superior to all other methods considered in this study because it predicted the ultimate failure load of all specimen groups with cracks embedded in the adherends without encountering singularity error. The mathematical linear progressive failure analysis is also carried out for understanding the failure mode in both adherends and adhesive layers, which is in agreement with the reported experimental findings. Therefore, Bond EM is suitable for estimating the ultimate failure load of ABC joints in a global or large size one and two-dimensional finite element model with and without composite ply delamination/crack induced due to various reasons. This method is practically adaptable by the composite structural designer for understanding the structural behavior of large composite aircraft parts with manufacturing defects and damages. So far, Bond EM predicted the failure load of *12* experiments of third-party specimens and compared it with *eight* other theoretical and numerical failure load estimation methods. The authors have formulated mathematical equations and carried out analytical studies. All test results are considered from other references.

Acknowledgments

The authors have carried out this analytical study using the available infrastructures of CSIR-NAL Bengaluru, an aerospace research and design organization funded by the Government of India.

Therefore, no claims and conflicts from others involved in this study. The contribution of Ms. Dixi Patel is acknowledged.

References

[1] James Polagangu, K. Mahesh, Varghese Byji, "Estimation of failure load of composite bonded joints using 1D and 2D FE analysis and the mathematical equation of strain and bond energy in the adhesive layer", Mechanics of Advanced Materials and Structures, 2019, Vol. 26, Issue 1, pp: 20-28. https://doi.org/10.1080/15376494.2018.1516254

[2] L. Tong. Failure of Adhesive-Bonded Composite Single Lap Joints with Embedded Cracks. J. AIAA, Vol. 36, No 3, March 1998. https://doi.org/10.2514/2.385

[3] Mohammad Kashfuddoja., M, Ramji. Whole-field strain analysis and damage assessment of adhesively bonded patch repaired CFRP laminates using 3D-DIC and FEA. J. Composite. Part B, 53 (2013), 46-61. https://doi.org/10.1016/j.compositesb.2013.04.030 https://doi.org/10.1016/j.compositesb.2013.04.030

[4] Kumari Asha, Byji Varughese, D. Saji. Stress analysis of stepped lap bonded repair joint under compressive loading. Proceedings of ISAMPE National Conference on Composites INCCOM-12, CP160 (2013). Bangalore, India.

[5] Zong-Hong Xie., Xiang Li., Sui-An Wang. Parametrical study on stepped-lap repair of composite laminates. The 2016 Structures Congress. Structures16. Jeju Island, Korea.

[6] Phil Yarrington, James Zhang and Craig Callier. Failure Analysis of Adhesively Bonded Composite Joints. 46th AIAA/ASME/ASCE/AHS/ASC/ Structures, Structural Dynamics & Material Conference, 18-21 April 2005, Austin, Texas. https://doi.org/10.2514/6.2005-2376

[7] M. J. Hinton, A. S. Kaddour, P. D. Soden. A Comparison of the Predictive capabilities of current Failure Theories for Composite Laminates, Judged against Experimental Evidence. Composites Science and Technology 62 (2002) pp: 1725-1797. https://doi.org/10.1016/S0266-3538(02)00125-2

[8] Polagangu James, Byji Varughese, Ramesh Sundaram. Analytical qualification of composite co-cured T-Joint for the internal fuel pressure requirement using a novel FE analytical approach: Bubbles in Bermuda Triangle. CPID-8, SL. No 19, INCCOM-16: ISAMPE-National Conference on Composites.September 20-21, 2019, Mascot Hotel, Thiruvananthapuram, Kerala, India.

[9] https://www.britannica.com/science/mechanics-of-solids#ref611523.

[10] https://www.britannica.com/science/mechanics-of-solids/History.

[11] S P Timoshenko. History of strength of materials. McGraw-Hill New York,1953.